*URSI GASS 2020, Rome, Italy, 29 August - 5 September 2020*

# Performance of Electric Near-Field Probes for Immunity Tests

Xinglong Wu*(1), Flavia Grassi(1), Sergio A. Pignari(1), Umberto Paoletti(2), and Isao Hoda(2)
(1) Dept. of Electronics, Information and Bioengineering, Politecnico di Milano, Milan, Italy
(2) Reliable Electronic Systems Research Dept., Hitachi, Ltd. Research & Development Group, Yokohama, Japan

## Abstract

This work investigates the performance of electric near-field probes, either realized by PCBs or semi-rigid coaxial cables, for immunity testing at PCB level. To this end, full-wave simulations and measurements are exploited to thoroughly investigate the performance of the probes in terms of coupling effectiveness, spatial resolution, impact of probe-to-trace gap, and rated power. Advantages and limitations of the two types of probes are eventually discussed.

## 1 Introduction

Electronic components and traces on printed circuit boards (PCBs) both emit and receive electromagnetic (EM) noise. The requirement of integrating an increasing number of components in a confined volume triggers issues related to near-field coupling, which results to be detrimental as far as intra-system compatibility is the target.

To identify and troubleshoot such interference effects, near-field scan methods have been introduced firstly for measurement of EM emissions [1] and then for EM immunity tests [2]. In this technique, the design of suitable near-field probes plays a key role, since the specific probe structure and position determine the coupling with the PCB under test. In recent years, several research groups have designed and developed probes for near-field testing, [3-7]. However, in spite of the large variety of electric near-field (E-field) probes, two main probe categories can be identified, i.e., PCB-based probes and semi-rigid coaxial probes.

This work is aimed at investigating and comparing the performance of such probe structures in the framework of electromagnetic compatibility verification, with a specific focus on immunity tests. To this end, two near-field E-probes (one PCB-based and the other exploiting a semi-rigid coaxial cable) were considered and tested on *ad hoc* conceived PCBs [8]. The coupling effectiveness is quantified in terms of transmission S-parameter between the input port of the probes and the output terminals of the microstrip line under test. A systematic comparison is carried out for different configurations. By the light of the obtained results, pros and cons of the two E-field probe designs are outlined.

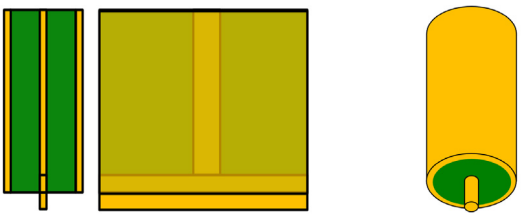

(a) (b)

**Figure 1**. Principle drawing of the tip of (a) PCB-based probes, and (b) semi-rigid coaxial cable probes.

## 2 Near-Field Probes under Analysis

### 2.1 PCB-based probes

The specific layout of PCB-based probes depends on designers and manufacturers. However, in general, the PCB stack-up should involve at least 3 layers. Both top and bottom layers are copper planes for grounding and EM shielding. The inner layer(s) hosts strip-lines for signal transmission, often realized as open-ended straight lines in E-field probes, and U-type loops in H-field probes. A principle drawing of the tip of the commercial PCB-based E-field probe considered in this work (i.e., probe RFE10, [9]) is shown in Fig. 1(a).

### 2.2 Semi-rigid coaxial probes

Alternatively, E-field probes can be realized by the use of semi-rigid coaxial cables left open-ended at one extremity, and equipped with a connector (e.g., an SMA connector if the frequency interval of interest is up to a few of GHz). A principle drawing is shown in Fig. 1(b), where the inner wire is kept longer than the probe main body to create a tip. The electric near-field probe considered in this paper was realized by using a semi-rigid coaxial cable RG405, with a 1 mm tip.

## 3 Performance of PCB-based and Coax Probes

In this Section, the performances of PCB-based and coaxial probes are investigated and discussed. To this end, the *S*-parameters of the test setup depicted in Fig. 2 are predicted by using Ansys HFSS. The line consists of two straight copper traces (length $L = 149$ mm, width $w = 0.15$ mm and thickness $t = 18$ μm) on top of a dielectric substrate with

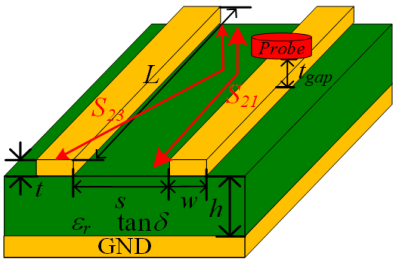


**Figure 2**. 3D view of the setup under analysis.

the following parameters: thickness $h$ = 70 µm, relative permittivity $\varepsilon_r$ = 3.4, and loss tangent tan$\delta$ = 0.001. The characteristic impedance ($Z_c$) is 49.3 Ω. The trace separation, $s$, is either 2 mm or 0.3 mm. The probe is placed on the middle of one trace with a 0.02 mm air gap ($t_{gap}$) between metal tip of the probe and the trace under test.

The $S$-parameters $S_{21}$ and $S_{23}$ are considered. $S_{21}$ provides a measure of the coupling between the probe and trace under test. $S_{23}$ represents the coupling between the probe and the nearby trace, and it is used as a measure of the probe spatial resolution. For the two probes under analysis, predictions of $S_{21}$ and $S_{23}$ obtained for different trace separations are compared in Fig. 3.

## 3.1 Coupling between the probe and trace under test

Fig. 3(a) clearly indicates that the presence of additional traces in close proximity to the trace under test does not influence the coupling coefficient ($S_{21}$) between the probe and the trace under test. The comparison between different probes shows that the PCB-based probes can provide higher coupling (+ 5.6 dB at low frequency) than the coaxial probe, on condition the probe-to-trace distances are the same.

This conclusion, drawn on the basis of numerical simulations, does not account for the fact that in practical realizations, the tips of commercial PCB-based probes are usually covered by dielectric material for protection and isolation. Hence, the actual distance between the probe tip and the trace under test may be larger for these probes than for hand-made coaxial probes, with a consequent decrease of the corresponding coupling coefficient, as the measurement presented in Sec. IV will illustrate.

## 3.2 Spatial resolution

The S-parameter $S_{23}$ in Fig. 3(b) allows appreciating the influence of trace separation on spatial resolution. At low frequency, the difference between the two curves pertinent to the coaxial probe is significantly larger than that for the PCB-based probe. This indicates that PCB-based probes generally offer better spatial resolution than coaxial probes. Indeed, as shown in Fig. 1, PCB-based probes are designed to assure field directivity, while semi-rigid coaxial probes do not.

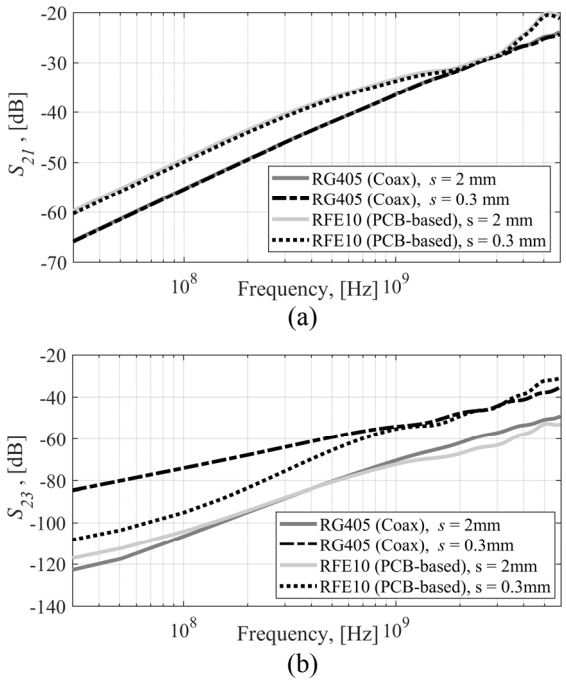


**Figure 3**. Impact of trace separation. Coaxial (RG405) probe vs PCB-based (RFE10) probe: (a) $S_{21}$; (b) $S_{23}$.

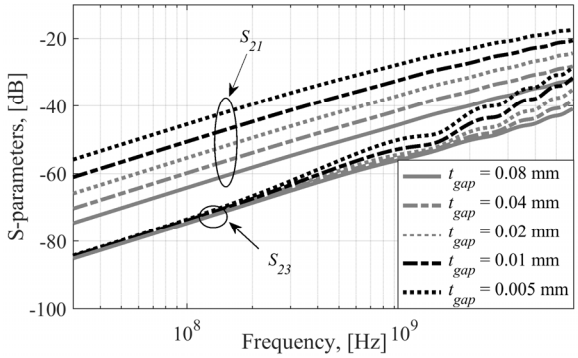


**Figure 4.** Coaxial probe: impact of the distance between the probe tip and the trace under test.

## 3.3 Influence of the probe-to-trace distance

The distance between the probe tip and the trace under test is a key parameter to determine coupling effectiveness. As previously mentioned, the tips of PCB-based probes are usually covered by dielectric material, which significantly contributes to increasing the actual distance between the probe tip and the trace under test. On the other hand, it should be considered that such an insulation allows placing the probe in contact with any PCB trace or pin even in the absence of the solder mask. This is no longer true when considering coaxial probes. As a matter of fact, since these probes are usually hand made, their bare tip should be kept at a certain minimum distance from the trace under test, in order to avoid metallic contact (in case the solder mask is not present).

To investigate the influence of such a tip-to-trace air gap on the coupling performance of coaxial probes, a set of configurations with $s$ = 0.3 mm and different $t_{gap}$ was

simulated. The obtained *S*-parameters are plotted in Fig. 4. It is observed that for $t_{gap}$ two-times larger, the coupling coefficient ($S_{21}$) decreases by 4.5~5 dBs, which is line with the observation that probe-to-trace coupling is mainly capacitive. The same comparison for $S_{23}$ reveals that $t_{gap}$ does not appreciably influence the coupling with nearby traces at low frequency, at least as long as trace separation is much larger than the probe tip length.

### 3.4 Maximum power for immunity tests

For immunity testing especially in continuous wave (CW), an important parameter to be considered is the maximum power the probe can withstand without damages. In this respect, resorting to traditional PCB-based probes for CW injection may pose stringent limitations in terms of power. As a matter of fact, to the best of Authors' knowledge, the maximum forward power suggested for commercial PCB-based E-field probes is in the order of 5 W (at least up to 1 GHz), e.g., [9]. Conversely, exploiting coaxial probes offers more flexibility in terms of maximum power. For instance, for a hand-made probe realized by means of an RG405 semi-rigid coaxial cable, the maximum power can be roughly in the order of 35 W (for frequencies below 10 GHz), [10].

## 4 Measurement

In order to validate numerical predictions of the probe coupling coefficient and to investigate practical issues not put in evidence by full-wave simulations, a PCB sample was fabricated with a 149 mm long microstrip line with 0.15 mm width (see Fig. 5(a)). Geometrical and material characteristics of the FR4 substrate are: $h = 80$ µm, $\varepsilon_r = 4.7$, $\tan\delta = 0.014$, $t = 35$ µm. The corresponding characteristic impedance $Z_c$ is 45 Ω. The trace is covered by a FR4-based solder mask with nominal thickness $t_{mask}$ = 0.03mm. For measurement, the two probes were placed on top of the trace at midpoint, by using a manual positioner ($t_{gap}$ = 0 mm), as shown in Fig. 5(b) and Fig. 5(c).

The coupling coefficient $S_{21}$ was simulated in Ansys HFSS and measured by using a Vector Network Analyzer (VNA) Keysight E5071C. The results are compared in Fig. 5(d), showing excellent agreement between simulation and measurement up to 6 GHz. Here, the PCB-based probe has a slightly less $S_{21}$ than the coaxial probe. This is because this PCB-based probe tip is prevented by covering it with a dielectric coat, which, actually, increases the probe-to-trace gap.

To experimentally investigate probe performance also in terms of spatial resolution, an additional PCB was used with a bare, i.e., without solder mask, pair of microstrips printed on top of double-face PCB [8]. The PCB is 1.6 mm thick with FR4 substrate material. Trace thickness, length and width are 35 µm, 280 mm and 1 mm, respectively. The two traces are separated by 2 mm. The two probes were placed on one of the two traces at midpoint, as presented in Fig. 6 (b) and (c). It is worth mentioning that, unlike

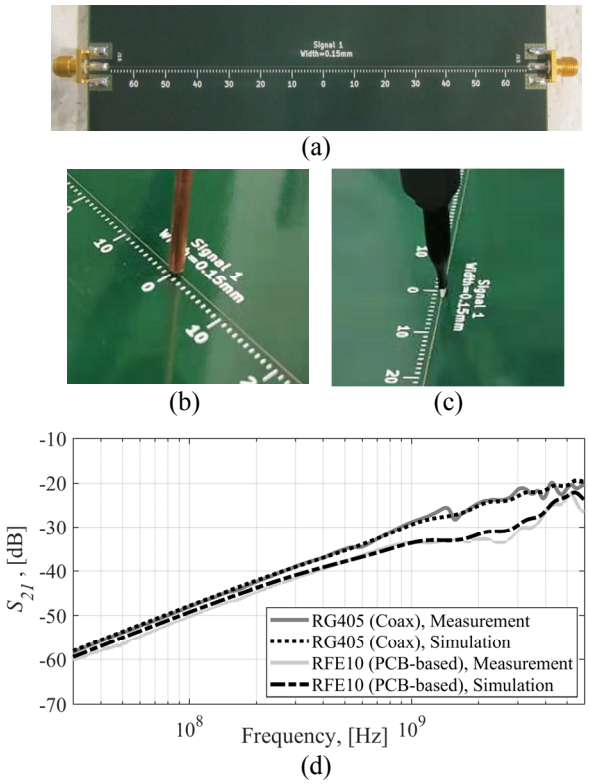


**Figure 5.** Experimental validation of coupling effectiveness: (a) PCB under test; (b) test example of coax probe; (c) test example of PCB-based probe; (d) measurement versus simulation.

previous tests where PCB traces were covered by the solder mask, here, the use of a thin plastic sheet (0.1 mm thickness) placed between the coaxial probe tip and trace is necessary to avoid direct contact, see Fig. 6 (b)). Conversely, this measure is not required for the PCB-based probe thanks to the dielectric coat covering its tip.

The measurement results in Fig. 6 (d) and (e) indicate that the PCB-based probe has better coupling effectiveness ($S_{21}$) but similar spatial resolution ($S_{23}$) in the frequency range 30 MHz~1 GHz. Conversely, both $S_{21}$ and $S_{23}$ of the PCB-based probe are generally smaller than those of the coaxial one from 1 GHz to 6 GHz.

## 5 Discussion

Based on the above investigation, the following pros and cons of PCB-based probes and coaxial can be outlined.

The accurate design of PCB-based probes, on the one hand, usually provides better theoretical coupling effectiveness and field directivity, but on the other hand, it involves a strict power limitation. In addition, a thin dielectric coat covers tips of PCB-based probes, which makes it convenient to be applied in any noncontact tests. This is significantly important for automatic tests of sensitive PCBs because some automatic positioners measure the probe-to-trace gap by touching the probe to trace under test. Of course, this coat also makes this type of probes non-available for contact tests.

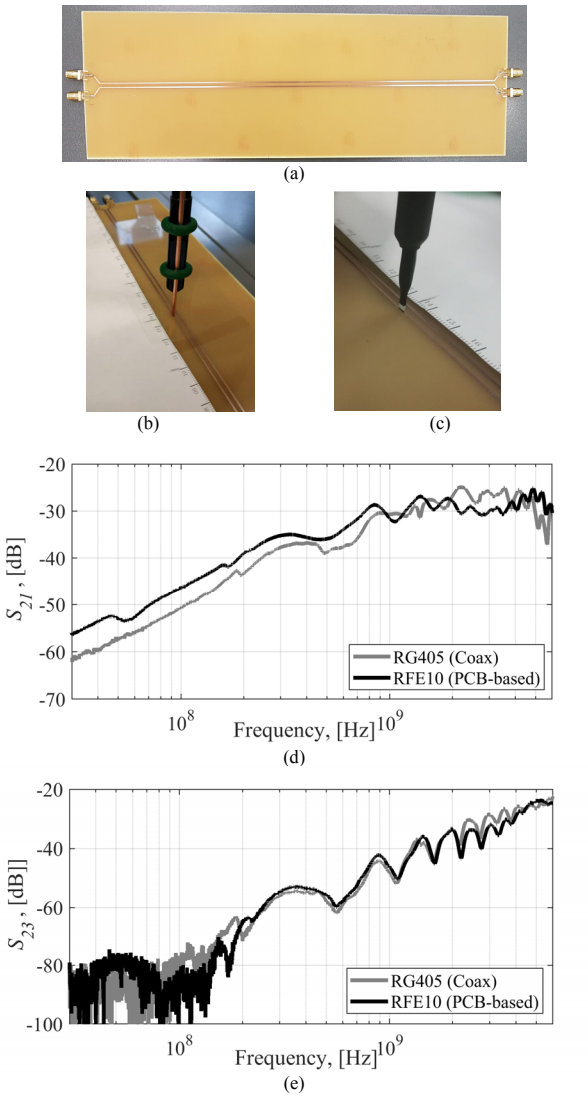


**Figure 6**. Test on a differential line: (a) PCB under test; (b) test example of coax probe; (c) test example of PCB-based probe; (d) measurement versus simulation.

On the contrary, thanks to its open metal tip, coaxial probe can be used for contact tests. Furthermore, in noncontact tests, it can be directly placed on the solder mask, which shortens probe-to-trace gap and sometimes gives better coupling effectiveness. Its coupling increases linearly with frequency, making it easier to be modeled in circuit simulators. Furthermore, it has much higher rated power, which is a big plus in immunity tests. However, coaxial probe does not have field directivity and should be used very carefully in noncontact tests to avoid unwanted metallic connection between probe and trace.

## 6 Conclusion

This work presents a systematic investigation of the performance of PCB-based and hand-made coaxial E-field probes when used as injection devices for immunity tests. The probe coupling effectiveness, spatial resolution, and rated power are considered as figures of merit to evaluate pros and cons of the two design strategies, for EM susceptibility verification. Two experimental examples were provided to validate the accuracy of numerical simulations and to display their practical performance on different PCBs under test. Finally, a systematic comparison between the two types of probes was given, showing their advantages and limitations in immunity tests.

## 7 References

1. International Electro-Technical Commission IEC TS 61967-3: Integrated Circuits - Measurement of radiated emission - Part 3: surface scan method, 2014.

2. International Electro-Technical Commission IEC TS 62132-9: Integrated Circuits - Measurement of Electromagnetic Immunity - Part 9: surface scan method, 2014.

3. D. Baudry, C. Arcambal, A. Louis, B. Mazari, and P. Eudeline, "Applications of the near-field techniques in EMC investigations," *IEEE Trans. Electromagn. Compat.*, **49**, 4, Nov. 2007, pp. 805–815, doi: 10.1109/TEMC.2007.902194.

4. G. Muchaidze, J. Koo, Q. Cai, T. Li, L. Han, A. Martwick, K. Wang, J. Min, J. L. Drewniak, and D. Pommerenke, "Susceptibility scanning as a failure analysis tool for system-level electrostatic discharge (ESD) problems," *IEEE Trans. Electromagn. Compat.*, **50**, 2, May 2008, pp. 268–276, doi: 10.1109/TEMC.2008.921059.

5. Z. Yan, W. Liu, J. Wang, D. Su, X. Yan and J. Fan, Sensitivity and Spatial Resolution for Noise Location on PCB," *IEEE Trans. Instrum. Meas.*, **67**, 12, Oct. 2018, pp. 2881–2891, doi: 10.1109/TIM.2018.2830859.

6. J. Shepherd, C.Marot, B. Vrignon, and S. B. Dhia, "Near-field scan—State of the art and standardisation," in *Proc. Asia–Pacific Symp. Electromagn. Compat. (APEMC)*, Singapore, Singapore, May 2012, pp. 1–4, doi: 10.1109/APEMC.2012.6237881

7. A. Durier, S. B. Dhia and T. Dubois, "Comparison of voltages induced in an electronic equipment during far field and near field normative radiated immunity tests," in *Proc. Symp. Electromagn. Compat. Europe*, Sep. 2–6, 2019, Barcelona, Spain, pp. 938–943, doi: 10.1109/EMCEurope.2019.8871798

8. F. Grassi, Y. Yang, X. Wu, G. Spadacini, S. A. Pignari, "On mode conversion in geometrically unbalanced differential lines and its analogy with crosstalk," *IEEE Trans. Electromagn. Compat.*, **57**, 2, Apr. 2015, pp. 283-291, doi: 10.1109/TEMC.2014.2372894.

9. RFE10, Langer RF E10 probe, Langer EMV-Technik, [Online]. Available: https://www.langer-emv.de

10. RG405, Infinite Electronics International, Inc. [Online]. Available: https://www.pasternack.com